Electronic structure of NPB and BCP molecules probed by x-ray emission spectroscopy

J. H. Seo and C. Y. Kim
Institute of Physics and Applied Physics, Yonsei University, Seoul 120-749, Korea

S. J. Kang
Department of Materials Science and Engineering, University of Illinois at Urbana Champaign, Urbana, Illinois 61801

K.-H. Yoo and C. N. Whang
Institute of Physics and Applied Physics, Yonsei University, Seoul 120-749, Korea

A. Moewes and G. S. Chang[a)]
Department of Physics and Engineering Physics, University of Saskatchewan, Saskatoon, SK S7N 5E2, Canada

(Received 14 August 2006; accepted 9 January 2007; published online 13 February 2007)

Soft x-ray absorption and emission spectroscopies have been employed to investigate the electronic structure and chemical bonding of two prototypical molecules, N,N'-bis-(1-naphthyl)-N,N'-diphenyl-1,1′-biphenyl-4,4′-diamine (NPB) and bathocuproine (BCP), which are frequently chosen because of their hole-transporting and hole-blocking properties, respectively. The resulting resonant C $K\alpha$ x-ray emission spectra of these materials reveal different spectral features depending on the resonant excitation energy. According to the N absorption and emission spectra, the contribution of N atoms to the highest occupied and lowest unoccupied molecular orbitals is different for in NPB and in BCP. Detailed knowledge of these materials will allow tailoring charge transport properties of organic devices in order to develop high performance organic light-emitting diodes and photovoltaic cells. © *2007 American Institute of Physics*. [DOI: 10.1063/1.2464086]

I. INTRODUCTION

Light-emitting diodes and photovoltaic cells based on organic materials have been studied as potential applications in next-generation optoelectronic and solar-energy conversion devices since Tang and VanSlyke reported an efficient electroluminescence from organic thin bilayers (aromatic diamine/8-hydroxyquinoline aluminum) and an improved photovoltaic response from an organic *p-n* heterojunction cell (a copper phthalocyanine/perylene tetracarboxylic derivative).[1,2] Subsequent research efforts were devoted to enhance the electronic characteristics of organic devices such as light-emitting efficiency, charge-carrier mobility, power-conversion efficiency, and long-term chemical stability.[3–5] Regarding these enhancements in organic light-emitting diodes (OLEDs) and organic solar cells (OSCs), one of the widely used methods is the introduction of additional buffer layers. Bathocuproine (BCP) and N,N'-bis-(1-naphthyl)-N,N'-diphenyl-1,1′-biphenyl-4,4′-diamine (NPB) played an important role in this approach due to their efficient hole/exciton-blocking and hole-transport properties, respectively. For instance, Huang *et al.* increased the forward external quantum efficiencies significantly (~4.5% at 10–15 V bias) by using the BCP and NPB layers in the tris(8-hydroxyquinoline) aluminum(III)/1% di-isoamylquinacridone-based OLEDs.[3] It has also been reported that a BCP layer has been inserted between blue-emitting N,N'-bis-(1-naphthyl)- N,N'-diphenyl-1,1′-biphenyl-4,4′-diamine (NPB) and ovaline-emitting aluminum tris(8-hydroxyquinoline) in order to produce white light emission.[6] BCP has been also applied to develop efficient OSCs. Ahn *et al.* reported that the insertion of BCP between fullerene layer and Al cathode significantly enhances the quantum efficiency of conjugated polymer/fullerene heterojunction solar cells.[7]

Although it is essential to know the detailed bonding configurations of the constituent elements (especially carbon and nitrogen) in order to understand their hole-transporting (NPB) and hole-blocking (BCP) properties, the electronic structure of these materials has not been studied in detail.

In this paper, we employ soft x-ray absorption spectroscopy (XAS) and x-ray emission spectroscopy (XES) to investigate the electronic structure of C and N atoms in NPB and BCP molecules. Localized transitions in x-ray absorption and emission processes occur in the first coordination sphere of the excited atom, and thus XES and XAS probe the partial electronic structure of the constituent elements in organic molecules in element-specific fashion.[8] The measured XAS and XES spectra of NPB and BCP molecules are compared to our theoretical density of states (DOS) calculated by density functional theory (DFT).

II. EXPERIMENT

100 nm thick NPB and BCP films were thermally evaporated onto a SiO_2 layer, which is synthesized on a heavily

[a)]Author to whom correspondence should be addressed. Electronic mail: chang@usask.ca

doped silicon substrate by a dry oxidation process. Base pressure and deposition rate were maintained at 1×10^{-9} Torr and 0.1 Å/s, respectively. After an *in situ* preparation of the NPB and BCP films, a 5 nm thick Au capping layer is deposited (without breaking the vacuum) in order to avoid the sample contamination.

The unoccupied and occupied C $2p$ partial DOSs of the NPB and BCP films were probed by employing soft x-ray absorption and emission spectroscopies, respectively. All experiments were carried out at Beamline 8.0.1 of the Advanced Light Source at the Lawrence Berkeley National Laboratory. The XAS measurements were carried out in the total electron yield mode. Excitation energies (E_{exc}) for the resonant and nonresonant C $K\alpha$ ($2p \rightarrow 1s$ transition) emission spectra were selected at 285.2 and 310 eV, respectively. N $1s$ XAS and nonresonant N $K\alpha$ emission spectra (excited at E_{exc}=435 eV) were collected as well. The measurement angle was maintained at 30° between the incident x-ray and the sample's surface normal. All measured spectra are normalized to the number of photons falling on the sample monitored by a highly transparent gold mesh.

III. RESULTS AND DISCUSSION

Figure 1(a) displays the C $1s$ XAS spectra of the NPB and BCP films as well as the spectrum of a reference sample of highly oriented pyrolytic graphite (HOPG). Since the electron transitions in x-ray absorption processes are governed by the dipole selection rule ($\Delta l = \pm 1$), the absorption spectra provide information about the partial density of carbon electronic states of p symmetry in the conduction band.[9] The peaks located at energies of 285.5 and 292 eV for HOPG correspond to $1s \rightarrow \pi^*$ and $1s \rightarrow \sigma^*$, respectively, which are typical for crystalline graphite.[10] On the other hand both NPB and BCP films show the π^* feature consisting of the intense peak around 285 eV and a small feature just above 284 eV, and the broad σ^* features spread over more than 7 eV while HOPG exhibits a more localized σ^* feature at 292 eV. These spectral behaviors of NPB and BCP films are due to the contribution from different benzene-ring complexes. As seen in Fig. 2, the NPB molecule consists of three kinds of benzene-ring complexes that are joined by two N atoms. One is a simple benzene ring—labeled C58–C63 in Fig. 2(a)—and the other two types are double-benzene-ring complexes in different arrangements and are labeled C1–C12 and C24–C35, respectively. The BCP molecule is composed of two benzene rings [C19–C26 in Fig. 2(b)] and one phenanthrene in which two C atoms are replaced with N atoms (C1 to C12).

The occupied carbon valence states of p symmetry of NPB and BCP are shown in Figs. 1(b) and 1(c). In the nonresonant C $K\alpha$ XES spectra of NPB and BCP films (solid line, excited at 310 eV), the spectral weight around 268–278 eV originates from σ states while that around 278–283 eV is assigned as π states. Although the NPB film has slightly higher π-emission states than the BCP film, NPB and BCP films both show the similar three-peak structure of carbocyclic aromatic rings (benzene).[11] This is due to the fact that both molecules consist of phenyl rings as building blocks. However, when the excitation energy is tuned to the π^* feature (open circle, excited at 285.2 eV), spectral differences become more distinct. The NPB film exhibits a strong resonant feature at 275 eV while other features around 278 and 281 eV are significantly suppressed under resonant excitation condition. These can be interpreted in terms of the parity selection rules for resonant x-ray scattering. When an electron is excited from a core orbital ($1e_{2g}$ orbital) to π^* state ($1e_{2u}$ orbital), the transition from any valence orbital with parity g to a $1e_{2g}^{-1}$ core hole would be symmetry forbidden due to the dipole character of resonant x-ray emission. The highest occupied molecular orbital (HOMO) states (spectral feature at 281 eV) and a feature at 278 eV are the $1e_g$ and $3e_{2g}+1a_{2u}$ orbitals, respectively. That is why NPB film shows a strong resonant feature at 275 eV which corresponds to x-ray transitions involving the $3e_{1u}+1b_{2u}+2b_{1u}$ orbitals. The result has a good agreement with resonant C $K\alpha$ XES spectra of benzene.[11] On the other hand the resonant structure at 275 eV is weaker in the BCP film because replacement of two C atoms in phenanthrene with N atoms results in modification of the σ-symmetry orbitals.

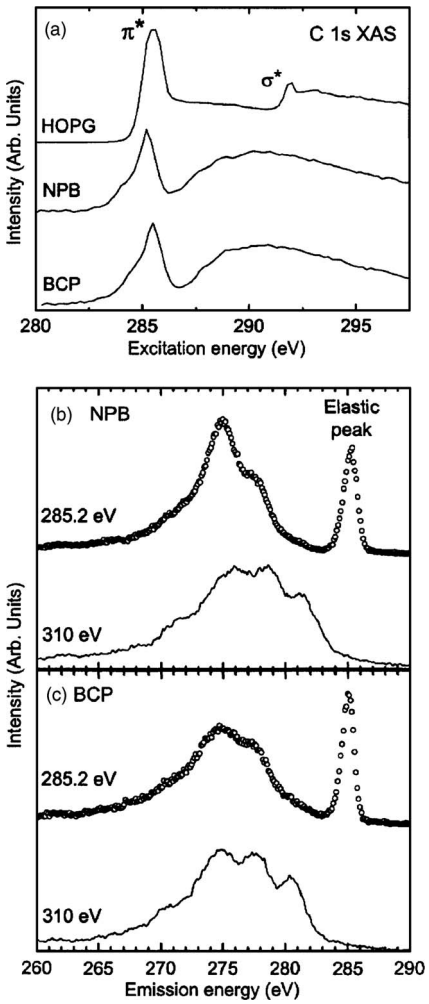

FIG. 1. C $1s$ XAS spectra of NPB, BCP, and HOPG (a), and C $K\alpha$ XES spectra of NPB (b) and BCP (c) measured at different excitation energies. To compensate for different amounts of C atoms in NPB and BCP films, the XES spectra taken at each excitation energy are normalized with the integral intensity ratio between NPB and BCP so that total XES intensity for NPB coincides with that for BCP.

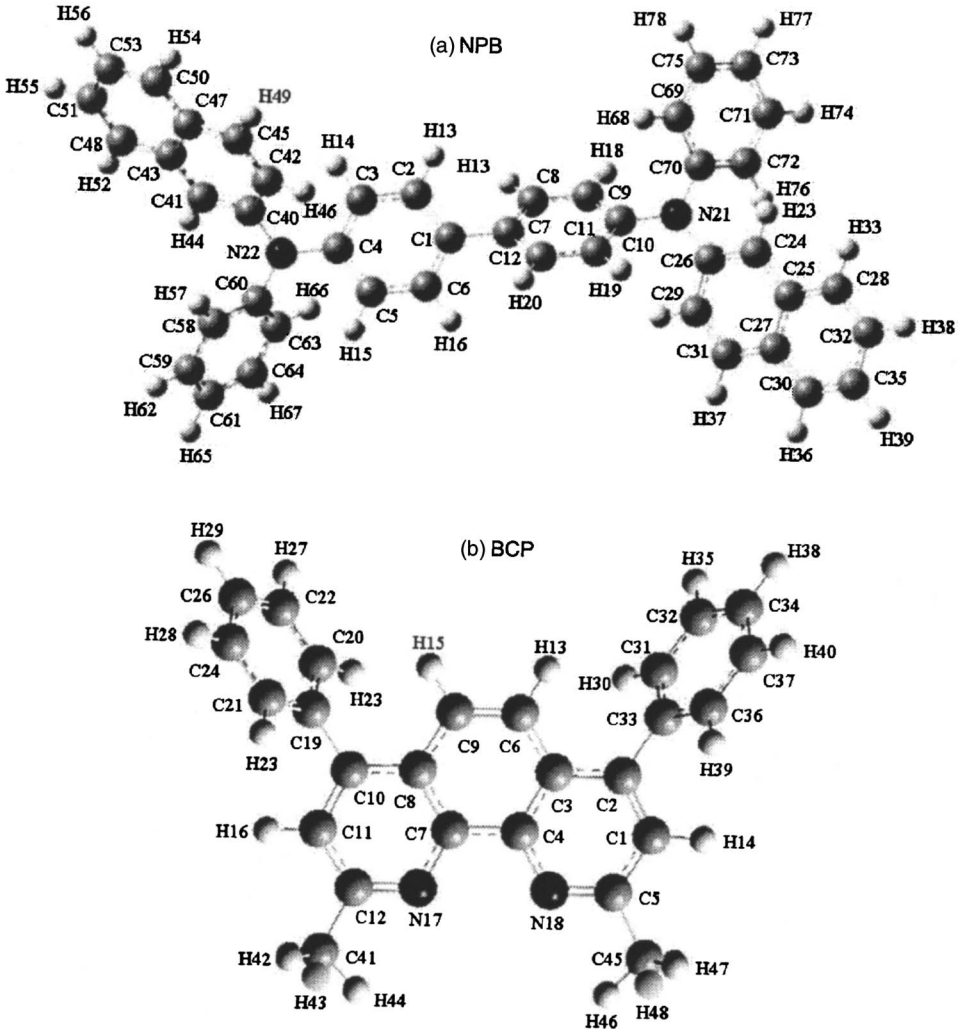

FIG. 2. Structural geometries of (a) NPB and (b) BCP molecules.

In addition to C 1*s* XAS and C $K\alpha$ XES spectra, we also measured N 1*s* XAS and nonresonant N $K\alpha$ XES spectra (excited at E_{exc}=435 eV), as displayed in Figs. 3(a) and 3(b), respectively. One can see that unoccupied π^* molecular orbital states significantly depend on different local environment around the N atoms in NPB and BCP. The N 1*s* XAS spectrum of the BCP molecule shows a dominant π^* feature at 401 eV, which is much weaker for the NPB molecule despite lower signal-to-noise ratio of the N 1*s* XAS spectra than that of the C 1*s* spectra which is due to the lower nitrogen content in both molecules. The N $K\alpha$ XES spectrum of the BCP [open circle in Fig. 3(b)] has slightly higher π valence states than the NPB film. The emission spectrum of the BCP resembles that of pyridine which has similar environment except one N–H bond.[12] Since the N atoms mediate a three-dimensional structure of organic semiconductors, the prominent difference in unoccupied π^* feature between BCP and NPB is related to the charge transferring properties of these molecules.

For further understanding of the spectral behavior of carbon and nitrogen XAS and XES spectra, DFT calculations were performed. We used the nonlocal hybrid Becke three-parameter Lee-Yang-Parr (B3LYP) function with a basis set of 6-31G. Before calculating the total DOS and projected DOS, the molecular geometries of the NPB and BCP were

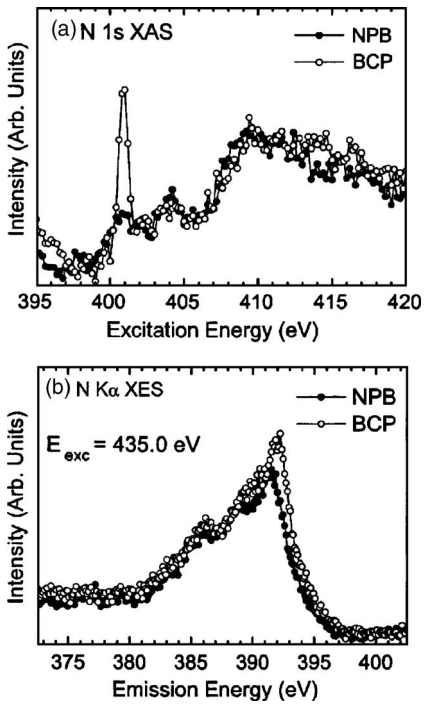

FIG. 3. (a) N 1*s* XAS spectra and (b) nonresonant N $K\alpha$ XES spectra (E_{exc}=435 eV) of NPB and BCP films.

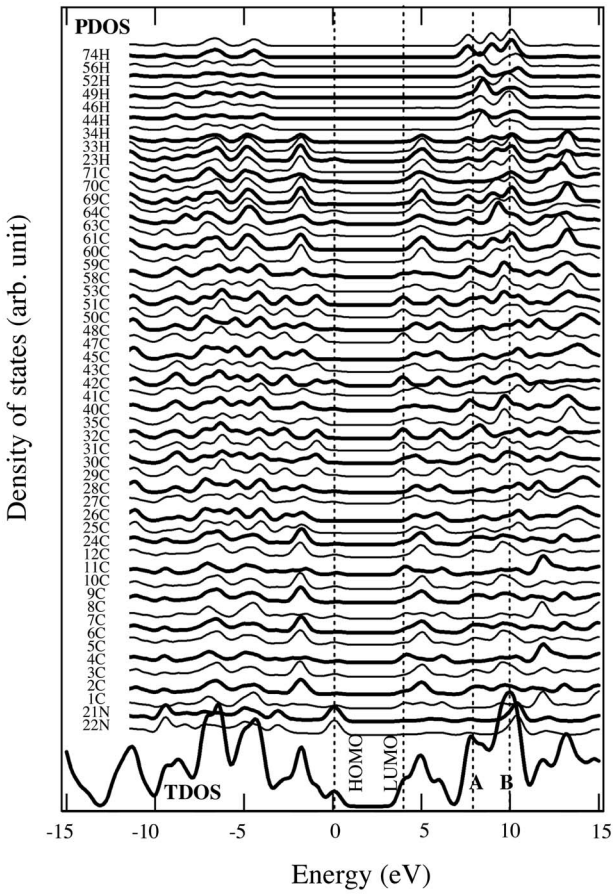

FIG. 4. Calculated total DOS and projected DOS of the NPB molecule.

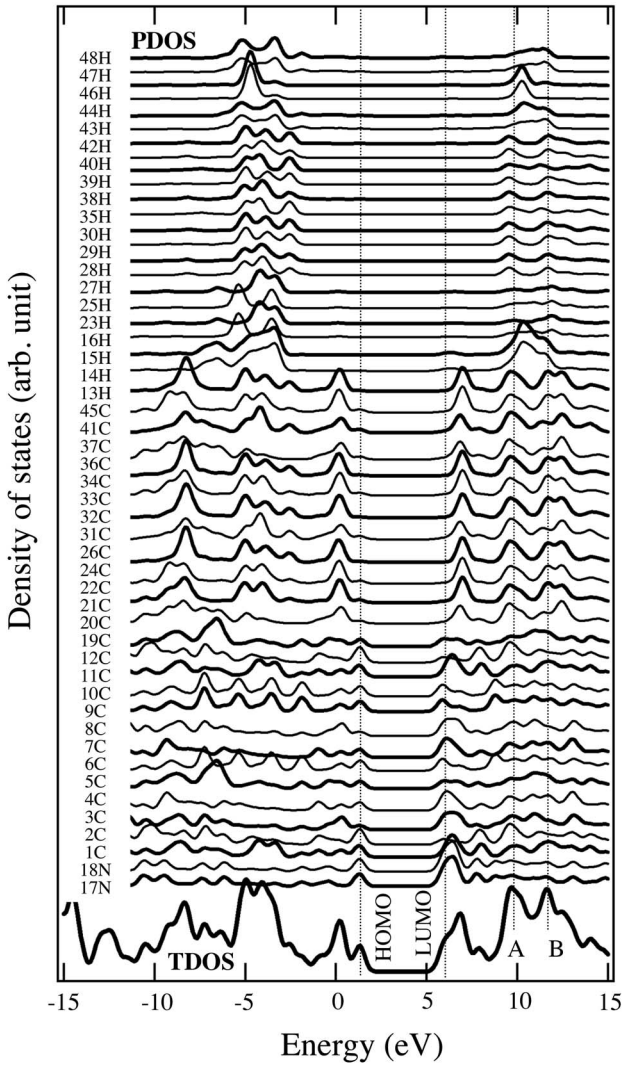

FIG. 5. Calculated total DOS and projected DOS of the BCP molecule.

optimized with the B3LYP/6-31G (Ref. 13) and the structures are presented in Fig. 2. From the obtained DOS, the spectra were broadened using a Gaussian function with a full width at half maximum of 0.1 eV. Figure 4 shows the total DOS of the NPB structure (thick solid line at bottom) as well as the projected DOS providing the information on the spectral contribution of all constituent atoms to the total DOS. The labeling of the atoms is the same as in Fig. 2(a). The overall spectral features agree well with the calculated electronic structure of the NPB molecule previously reported by Zhang *et al.*[14] By examining the projected DOS of the C and N (and H atoms), it is found that HOMO states of NPB have contributions mainly from N atoms. The lowest unoccupied molecular orbital (LUMO) states originate from C atoms in the two double-benzene-ring complexes [denoted by C24–C35 and C40–C53 in Fig. 2(a)] while simple benzene rings (C58–C63 and C69–C75) are responsible for intense conduction states just above HOMO position. The calculations well reproduce two spectral features at 284 and 285 eV in the C 1*s* XAS spectrum of NPB [Fig. 1(a)]. The broad spectral weight around 290 eV in the XAS spectrum stems from the superposition of two subpeaks in the conduction states (lines *A* and *B*). Otherwise the projected DOS of the H atoms resides in the energy range of 7–10 eV above the Fermi level and thus their contribution to the electric properties of NPB is negligible. The absence of N π^* states in the N 1*s* XAS spectrum shows a similar trend with the projected DOS of N atoms, which assists the good hole-transporting properties of NPB. As reported by Zhang *et al.*,[14] a hole injection of the NPB layer will excite an electron in N atom involving the HOMO states, and energetically excited N atom due to electron deficiency can be stabilized by the delocalized π characters of adjacent C atoms because the N atoms locate at the junctions of the conjugated C chains.

A similar analysis of the BCP molecule is presented in Fig. 5. Although BCP also consists of several benzene-ring complexes such as NPB, there are prominent differences in their electronic structure. The comparison of total DOS with the projected DOS reveals that the HOMO states of BCP are mainly composed by the N atoms and their neighboring C atoms in the phenanthrene [denoted by C1–C12 in Fig. 1(b)]. An interesting feature appears in the LUMO states. In contrast to NPB, the BCP molecule shows a significant contribution of the N atoms to the LUMO states (corresponding to the π^* feature in the experimental N 1*s* XAS spectrum). This indicates that upon the hole injection into the BCP layer, the excited π electron in the N atom to unoccupied π^* states will easily decay to the valence states and thus the N atoms in the BCP does not accept the hole from the active layer in OLED devices. On the other hand, C $K\alpha$ resonant inelastic x-ray

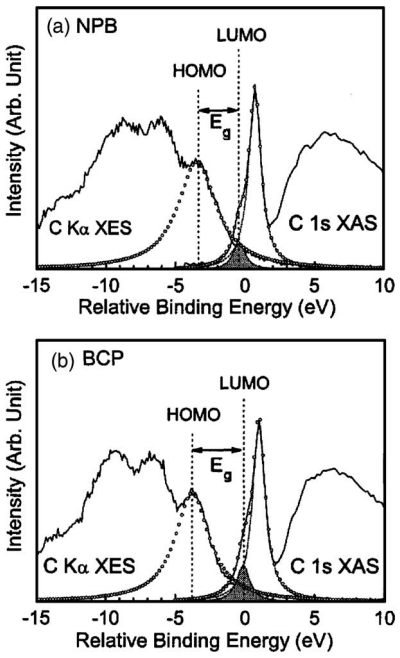

FIG. 6. C 1*s* XAS (solid line) and C *Kα* XES (filled circle) spectra of (a) NPB and (b) BCP films.

scattering spectrum for the BCP film suggests that the C atoms are not favorable sites for the hole injection and transport as well because more localized structure of the C atoms in BCP significantly restricts the hole movement through the benzene complexes.

In addition to the spectral differences between NPB and BCP discussed above, we attempted to estimate the HOMO-LUMO gap energies from displaying XES and XAS spectra on the same energy scale, as displayed in Figs. 6(a) and 6(b). The gap energy is one of the key parameters in applications of these materials to organic optoelectronics and photovoltaic cells. By assuming that neither the LUMO nor the HOMO levels shift perceptibly in the presence of a C 1*s* hole, the relative energies of XES and XAS spectra are calibrated using a C 1*s* binding energy of 284.5 eV. It is noted that these superposed spectra do not include the spectral contribution from the N atoms due to low signal-to-noise ratio of the N 1*s* XAS spectra but the projected DOS of the C atoms shows similar HOMO and LUMO energy positions with those of the N atoms. To determine the LUMO energy positions of NPB and BCP films, the π^* regions of C 1*s* XAS spectra were fitted by Lorentzian functions. The individual Lorentzian peaks (dotted line) and final fits (open circle) are displayed in Figs. 6(a) and 6(b), and then the peak maxima at −0.44 and −0.13 eV (shaded peaks) are assigned to be LUMO positions of NPB and BCP, respectively. Using a similar way, HOMO levels are determined from the positions of the rightmost peaks in C *Kα* XES spectra (−3.45 eV for NPB and −3.78 eV for BCP). The resulting HOMO-LUMO gap energies are about 3.01 eV for NPB and 3.65 eV for BCP. Although the accurate determination of the HOMO and LUMO positions depends on the spectral resolution of the XAS and XES spectra, the resultant gap energies for NPB and BCP films are in fair agreement with previously published results.[5,15,16]

IV. CONCLUSIONS

To conclude, the electronic structures of NPB and BCP molecules are studied by employing synchrotron-based x-ray absorption and emission spectroscopies as well as DFT calculations. It is found that different contributions of N and C atoms to the HOMO and LUMO states play an important role for the hole-transport properties of the NPB molecule. The compositions of HOMO and LUMO states derived from N atoms and the local electronic structure of C atoms in the benzene complexes suggest that the hole-blocking property of BCP can be attributed to the participation of N atoms in the HOMO and LUMO configurations and the localized bonding between C atoms. We note that the element- and momentum-selective XAS and XES techniques provide useful methods for evaluating electronic properties of organic materials.

ACKNOWLEDGMENTS

This work was supported by the Brain Korea 21 (BK21) project of the Korea Research Foundation (KRF) and the Korea Science and Engineering Foundation (KOSEF) through the National Core Research Center for Nanomedical Technology. Additional support by the Natural Sciences and Engineering Research Council of Canada (NSERC) and the Canada Research Chair program is gratefully acknowledged.

[1] C. W. Tang and S. A. VanSlyke, Appl. Phys. Lett. **51**, 913 (1987).
[2] C. W. Tang, Appl. Phys. Lett. **48**, 183 (1986).
[3] Q. Huang, J. Cui, J. G. C. Veinot, H. Yan, and T. J. Marks, Appl. Phys. Lett. **82**, 331 (2003).
[4] S. J. Kang, Y. Yi, C. Y. Kim, K.-H. Yoo, C. N. Whang, T. A. Callcott, K. Krochak, A. Moewes, and G. S. Chang, Appl. Phys. Lett. **86**, 232103 (2005).
[5] P. Peumans, A. Yakimov, and S. R. Forrest, J. Appl. Phys. **93**, 3963 (2003).
[6] J. Xiao, Z. B. Deng, C. J. Liang, D. H. Xu, and Y. Xu, Displays **26**, 129 (2005).
[7] Y. J. Ahn, G. W. Kang, C. H. Lee, I. S. Yeom, and S. H. Jin, Synth. Met. **137**, 1447 (2003).
[8] A. Augustsson, M. Herstedt, J.-H. Guo, K. Edström, G. V. Zhuang, P. N. Ross, Jr., J.-E. Rubensson, and J. Nordgren, Phys. Chem. Chem. Phys. **6**, 4185 (2004).
[9] P. Skytt, P. Glans, D. C. Mancini, J.-H. Guo, N. Wassdahl, and J. Nordgren, Phys. Rev. B **50**, 10457 (1994).
[10] R. A. Rosenberg, P. J. Love, and V. Rehn, Phys. Rev. B **33**, 4034 (1986).
[11] P. Skytt, J.-H. Guo, N. Wassdahl, J. Nordgren, Y. Luo, and H. Ågren, Phys. Rev. A **52**, 3572 (1995).
[12] E. Z. Kurmaev, A. Moewes, K. Endo, and D. L. Ederer, J. Electron Spectrosc. Relat. Phenom. **114–116**, 889 (2001).
[13] R. Q. Zhang, W. C. Lu, C. S. Lee, L. S. Hung, and S. T. Lee, J. Chem. Phys. **116**, 8827 (2002).
[14] R. Q. Zhang, C. S. Lee, and S. T. Lee, J. Chem. Phys. **112**, 8614 (2000).
[15] C.-C. Tsou, H.-T. Lu, and M. Yokoyama, J. Cryst. Growth **280**, 201 (2005).
[16] W. Gao and A. Kahn, J. Appl. Phys. **94**, 359 (2003).